Imaging of optical sparse aperture systems and its evaluation experimentally

Dayong Wang[1a], Ji Han [a], Xiyang Fu [b], Hongfeng Guo [b], Shiquan Tao [a]
[a]College of Applied Sciences, Beijing University of Technology, Beijing 100022, China
[b]National Astronomical Observatories , Chinese Academy of Science , Beijing 100012, China

ABSTRACT

Optical sparse aperture systems can be designed to obtain high resolution for imaging astronomical object. They are particular arrays synthesized by several small filled imaging systems. In this paper, a principle experiment is set up for optical sparse aperture system. Imaging of the extended complex object is achieved. Image restoration of the direct output by the sparse-aperture system is performed by measuring the point spread functions (PSF) and by using the Weiner filter. The correlation coefficient is proposed as a criterion to determine optimal parameter, and evaluate the performance of the algorithms. The results show that Tri-Arm array configuration among three kinds of configuration models can produce higher resolution and larger correlation coefficient value after restoration. Accordingly, based on the experimental data, the possibility is demonstrated that the optical sparse aperture systems can achieve almost the same resolution and image quality as an equivalent filled system.

Keywords: Optical imaging, Sparse aperture, Imaging system, Image restoration , High resolution

1. INTRODUCTION

With the development of Earth and Space missions, the quest for higher spatial resolution for telescopes will turn into urgent need. Particularly for space-based applications, the volume and mass constraints of current launched vehicles as well as the costs become increasingly prohibitive for telescopes with apertures greater than 1meter. Since the cost of monolithic optics increases faster than diameter squared, and mirrors such as the 10-meter ground-based systems and the 2.4-meter Hubble Space Telescope are already at the edge of what is financially feasible, efforts are ongoing to break this limit and this trend by employing breakthrough technologies[1-3]. Optical sparse aperture imaging system consists of many independent small aperture imaging systems, and the field-of-view (FOV) of this imaging system can achieve the FOV of the small aperture imaging system. In the FOV, when the outputs of each individual small aperture imaging system are overlapped and phased at the image plane, all the information below one spatial frequency in the object space can pass through the system, then the optical sparse aperture imaging system can realize almost the same resolution and image quality as an equivalent filled system in the view of information transfer.

Numerous research works have been paid to the optical sparse aperture imaging systems in the many countries because such systems not only obtain the same resolution and image quality as an equivalent filled system but also can reduce effectively the volume and mass as well as the costs of the system[1-13]. However, from the view of the practice, the optimization of the array configuration and the quantitative evaluation about the imaging performance based on the experimental data are not enough. In this paper, the experimental set-up is built as the principle optical sparse aperture system. Imaging of the extended complex object is performed. The digital restoration of the directly-output blurring images from the sparse aperture system is achieved by measuring the point spread functions (PSFs) with the CCD detector and by using the Weiner filter. Also, the correlation coefficient between two images is proposed as a criterion to evaluate the performance of the algorithms and the image quality. Firstly, in Section 2, with the equivalent model of the optical sparse aperture imaging systems, the modulation transfer functions (MTFs) and the PSFs are computed numerically for the three kinds of the typical array configuration. Also, the algorithms of the Wiener filter and the correlation coefficient are introduced. Next, in Section 3, the experimental set-up is described, and the measured PSFs and the corresponding MTFs are presented. The direct imaging of the United States Air Force (USAF) resolution target and their restoration are performed. The results show that the Tri-Arm array configuration among the three kinds of configuration models can produce higher resolution and larger correlation coefficient value after the restoration. Accordingly, based on the experimental data, the possibility is demonstrated that optical sparse aperture systems can achieve almost the same resolution and image quality as an equivalent filled system. Finally, we make the conclusions.

[1]wdyong@bjut.edu.cn; phone 86 10 67391741; fax 86 10 67392489; bjut.edu.cn

3rd International Symposium on Advanced Optical Manufacturing and Testing Technologies:
Large Mirrors and Telescopes, edited by Yudong Zhang, Wenhan Jiang, Myung K. Cho
Proc. of SPIE Vol. 6721, 672105, (2007) · 0277-786X/07/$18 · doi: 10.1117/12.782685

2. THEORY OF OPTICAL SPARSE APERTURE IMAGING SYSTEMS

2.1 Equivalent model of optical sparse aperture imaging system

Supposed that the sparse aperture imaging system is the space-invariant and incoherent imaging system, then the output of the imaging system can be written as [14]

$$I_i(x_i, y_i) = I_g(x_i, y_i) * PSF(x_i, y_i) \tag{1}$$

where,

$$PSF(x_i, y_i) = \left| F\{P(x, y)\} \right|^2, \tag{2}$$

"*" denotes the convolution operand, and $\mathrm{F}(*)$ is the Fourier transform operand. $I_i(x_i, y_i)$ is the intensity distribution of the directly produced image by the sparse aperture systems, $I_g(x_i, y_i)$ is the ideal image of the object predicted by the geometrical optics, $PSF(x_i, y_j)$ is the point spread function of the system, and $P(x, y)$ is the pupil function of the system. Eq. (1) can be rewritten in the frequency domain, as

$$\tilde{I}_i(f_x, f_y) = \tilde{I}_g(f_x, f_y) \bullet OTF(f_x, f_y) \quad , \tag{3}$$

where the functions in the above case are the Fourier transforms of the corresponding functions in Eq.(1). $OTF(f_x, f_y)$ is called the optical transfer function (OTF) of the system, which can be computed through the pupil function. If the system is diffraction-limited , the OTF is real and not negative, and itself is the modulation transfer function (MTF).

The pupil function for the optical sparse-aperture imaging system can be written as:

$$P(x, y) = P_0(x, y) * \sum_{n=1}^{N} \delta(x - \bar{x}_n, y - \bar{y}_n), \tag{4}$$

where, $(\bar{x}_n, \bar{y}_n)$ is the center coordinate of the nth small sub-aperture system, $P_0(x, y)$ is the sub-aperture pupil function of the system. In order to let all the frequency components pass through the system, the MTF usually need have no zero value below the cutoff frequency. In addition, the MTF value must be higher than some threshold value to meet the requirement of the signal-to-noise ratio (SNR) for the good imaging quality. It is necessary to arrange properly the relative positions of these small sub-aperture imaging systems, so that the array configuration is optimized.

2.2 Array configuration of optical sparse aperture imaging systems

The array configuration of the optical sparse aperture system decides the form of the pupil function, and then the distribution profile of the system MTF. There are three kinds of the typical array configurations of the sparse aperture systems, which are Annulus, Golay-6 and Tri-Arm, as shown in Fig. 1. Assuming that all of them have six small sub-apertures, we have calculated numerically the PSFs and the MTFs of each kind of the sparse aperture array by using Eq. (3) and (4), where the diameter of their equivalent filled system is 1 meter, and the focal length is 20 meter. For the simplification, the encircled diameter for the sparse aperture array is defined as the diameter of the overall aperture of their equivalent filled system. Fig. 2 and 3 show the PSF plots and MTF plots of the typical array configurations of the sparse aperture systems with the fill factor F of 30%. From the MTF plots, the pass band of the spatial frequency could be checked. For comparison, the MTF curves with two different fill factors (F=20% and 30%) are also given in Fig. 4, where the MTF curve of the equivalent filled system is also shown.

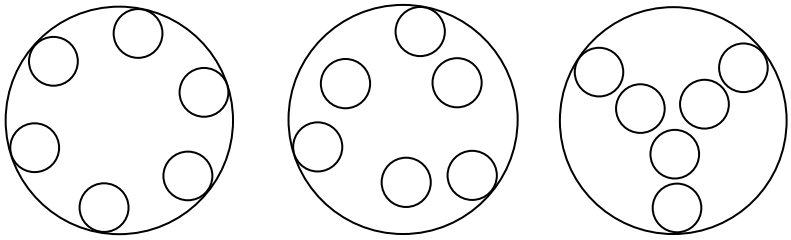

Annulus Golay-6 Tri_Arm

Fig.1 Three kinds of the typical array configurations of the sparse aperture systems

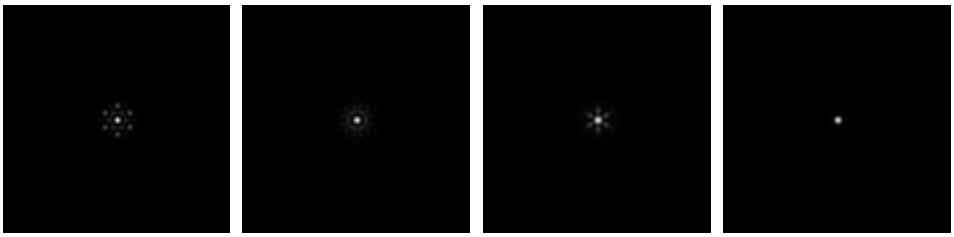

(a) Annulus (b) Golay-6 (c) Tri-Arm (d) Equivalent Filled

Fig.2 PSF plots of three kinds of the typical array configurations of the sparse aperture systems with F=30% and their equivalent filled system

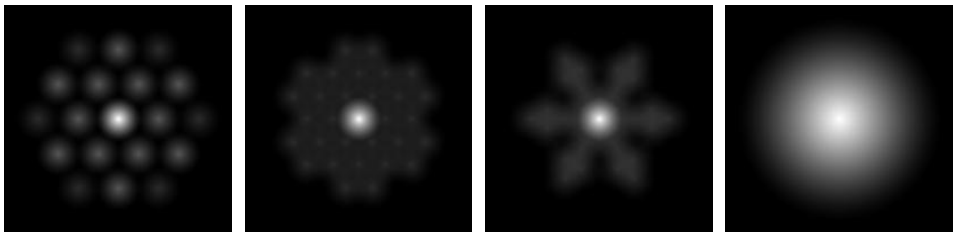

(a) Annulus (b) Golay-6 (c) Tri-Arm (d) Equivalent Filled

Fig.3 MTF plots of three kinds of the typical array configurations of the sparse aperture systems with F=30% and their equivalent filled system

Clearly, the MTF curves of three kinds of the typical array configurations of the optical sparse aperture imaging system always fall much more sharply than the equivalent filled system with the increase of spatial frequency. In the range of the middle and high frequency, the whole MTF curves are rather smooth with a little fluctuating. Especially, the values of MTFs of the optical sparse aperture imaging systems may be larger than the value of the MTF of the equivalent filled system at some high frequencies because the MTF is a normalized function. According to the MTFs, the direct imaging results of the optical sparse aperture systems would have the lower contrast than the image of the equivalent filled system. In other words, the directly-output image from the sparse aperture system should be blurring. Also, the MTFs for all the array configurations increase as the fill factor increases. However, the MTFs for the Golay-6 configuration and the Tri-Arm configuration will become more planar at the middle and high frequencies. The MTF for the Annulus configuration has the obvious fluctuating at the whole frequency range. With the fill factor of 20%, the zero value exists under the cutoff frequency of the MTF for the Annulus configuration. Since the smaller fill factor means the less sub-apertures and the light weight, it is preferable. But the MTF curve with the zero points under the cutoff frequency is not desired. Then it is necessary to make the compromise.

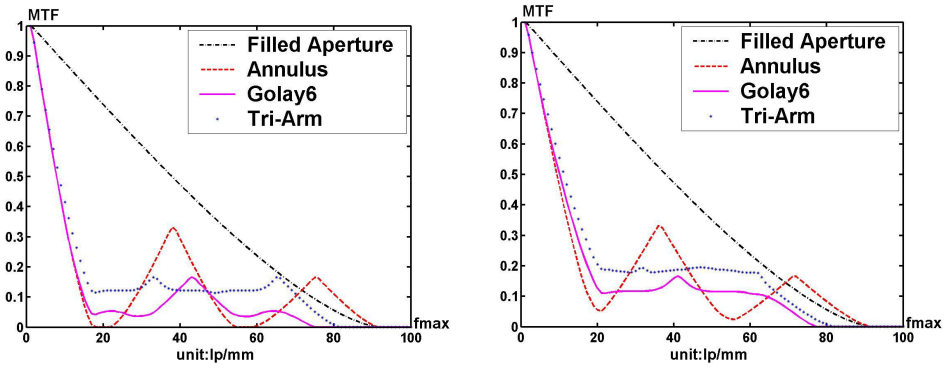

(a) F=20% (b) F=30%

Fig.4 MTF curves of three kinds of the typical array configurations of the sparse aperture systems and their equivalent filled system at the direction of the maximal cutoff frequency (Frequency unit: *lp/mm*)

2.3 Image restoration and its evaluation

The pupil function of the optical sparse aperture imaging system is partially filled with respect to the equivalent filled aperture, then the directly-output image of the system is blurring. In order to retrieve the image quality, an image restoration post-process is needed. Usually this is done in the frequency domain. For the Wiener filtering deconvolution, the transfer function of the filter has the following expression as[15]

$$W(f_x,f_y)=\frac{OTF^*(f_x,f_y)}{\left|OTF(f_x,f_y)\right|^2+\left|\frac{N(f_x,f_y)}{\tilde{I}_g(f_x,f_y)}\right|^2} \tag{5}$$

where $OTF^*(f_x,f_y)$ is the complex conjugate of $OTF(f_x,f_y)$ and $\tilde{N}oise(f_x,f_y)$ is the noise spectrum. For the practical space remote sense imaging, the final output may contain many factors in the imaging process, where some are random and uncertain. Then it is necessary to develop a quantitative evaluation to determine the restored image quality. Except for the resolution, it is proposed to use the correlation coefficient as a global criteria to evaluate the image quality and the performance of the algorithms. The correlation coefficient is defined as the following[15]

$$c=\frac{E\left[\left(f(x,y)-E[f(x,y)]\right)\left(\hat{f}(x,y)-E[\hat{f}(x,y)]\right)\right]}{\sqrt{E[f^2(x,y)]-\left(E[f(x,y)]\right)^2}\sqrt{E[\hat{f}^2(x,y)]-\left(E[\hat{f}(x,y)]\right)^2}}\ , \tag{6}$$

where, E[ ] denotes the mathematical expectation, $f(x,y)$ is the expected image, and $\hat{f}(x,y)$ is the restored image. When the correlation coefficient approaches 1 more closely, it shows that the restored image will be more similar to the expected image. It can be used to determine the optimal parameters, and to evaluate the performance of algorithms and the array configuration of the optical sparse aperture imaging systems by comparing the correlation coefficients between the different restored images and the ideal directly-output image.

3. EXPERIMENTS OF OPTICAL SPARSE APERTURE IMAGING

3.1 Experiment setup

The principle experimental setup for the optical sparse aperture imaging system is shown in Fig. 5. The quasi-monochromatic light source (green light) is produced by filtering the hydrargyrum (Hg) lamp. L_1 and L_2 are the doublelet lenses with the focal length of 84.1cm and the aperture diameter of 10cm. The United States Air Force (USAF)

resolution target is used as an extended object and placed at the focus plane of L_1. The sparse aperture mask is inserted between L_1 and L_2, and the distance between L_1 and L_2 is 75cm. In each mask, there are some small empty circle apertures with the same size, which are positioned according to the different array configurations. A high-resolution CCD detector, which has 1317×1035 pixels of 6.8μm×6.8μm size, is placed at the back focal plane of the lens. With this setup, some basic issues for the optical sparse aperture imaging could be studied, such as the optimization of the array configuration and the evaluation of the algorithm for the image restoration. The co-phasing condition among the independent small aperture systems would be satisfied automatically at the back focal plane of the lens L_2. Here the Annulus, Golay-6 and Tri-Arm array configurations are used and each has six small apertures. The corresponding aperture diameter of their equivalent filled system is 35mm. Also, two sets of the masks are prepared for each configuration with the fill factors of 20% and 30%. The corresponding diameters of the small circle apertures are 6.4mm and 7.8mm, respectively.

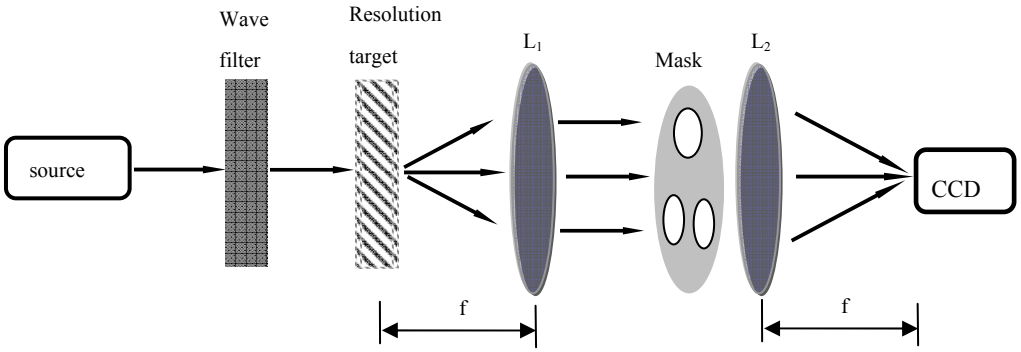

Fig.5 Experimental set-up of optical sparse aperture imaging system

3.2 Experimental process

There are three steps during the experiments. At first, the PSFs of the system are measured. That is to say, a pinhole with the diameter of 10μm will replace the extended target in the object plane as a point source. Then the image of the point source can be collected through the optical sparse aperture systems or their equivalent filled system by using the CCD detector. The detectable sensitivity of CCD usually can not be satisfied because of the low power of the Hg light source. So, the laser will be used as the illumination source to substitute for the Hg lamp, and the wavelength of the laser light is 532nm. It is necessary to correct the PSFs which is measured directly because of the coherent noise. Then, after doing the Fourier transform operation, the system MTFs can be obtained. The PSFs of the different optical sparse aperture systems are measured by inserting the different aperture masks into the setup, with the different array configurations and the fill factors, and so on. Then the corresponding MTFs will be achieved. Secondly, we will detect the direct image of the extended target for the different systems. In this step, the Hg light source is used as the illumination source. The USAF resolution target is put on the position as shown in Fig. 5 and used as the object. Then the direct output results of the optical sparse aperture imaging systems will be collected by the CCD detector. Finally, the restored images can be obtained by using the measured MTFs and the Weiner filter.

3.3 Experimental results

Based on the experimental data, the PSFs and the corresponding MTFs of the equivalent filled system and the optical sparse aperture systems are shown respectively in Fig. 6 and 7 at the fill factor of 30%. The MTF curves are given in Fig. 8 with the fill factors of 20% and 30%. By comparing the results of the numerical calculation and the results of the experimental data, the regularities of the distribution profile of the PSFs and the MTFs are similar. Due to the influence of some factors, for example, the practical devices and the environment, there exists just a little difference in details. In one word, the results of the experiments are coincident with the results of the theoretical prediction rather well.

The image through the equivalent filled aperture system is shown in Fig. 9. The direct images produced by the optical sparse aperture systems at the fill factor of 30% are blurring, as shown in Fig. 10 (a)-(c), corresponding to the Annulus, Golay-6 and Tri-Arm array configurations respectively. It is necessary to use the Weiner filter to restore the image. Here, Fig. 10 (d)-(f) shows the restored images which are placed below each directly output image. The results demonstrate that the image quality is improved after the restoration. The first line in the fifth group is still resolvable from the imaging result of the equivalent filled system, and the corresponding line width is 15.6μm. For the optical sparse aperture systems, the sixth line in fourth group can be distinguished from the imaging result with the Tri-Arm array configuration, and the corresponding line width is 17.5μm, and it is very close to the resolution of the equivalent filled system. In order to evaluate quantitatively the image quality of the extended complex target, the correlation coefficients between the imaging results of the equivalent filled system and the imaging results of the sparse aperture systems are calculated, as shown in Table 1. We can see that the correlation coefficients given by the restored images are much higher than given by the direct images. The Tri-Arm array configuration among the three kinds of the typical configuration models can produce higher resolution and larger correlation coefficient value after the restoration. And the optical sparse aperture systems can achieve almost the same resolution and the image quality as an equivalent filled system. Those are in accordance with the results of the numerical simulations.

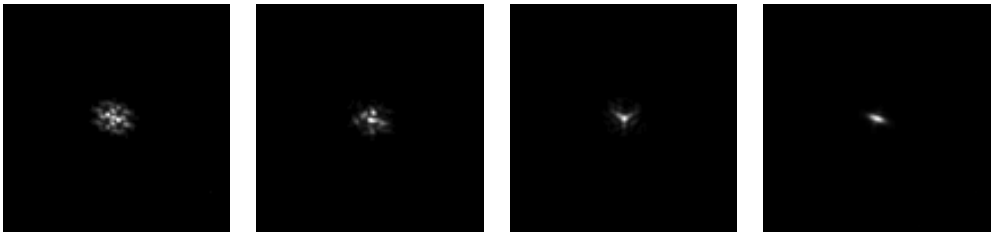

(a) Annulus (b) Golay-6 (c) Tri-Arm (d) Equivalent Filled

Fig.6 Measured PSF plots of three kinds of the typical array configurations of the sparse aperture systems with F=30 and their equivalent filled system

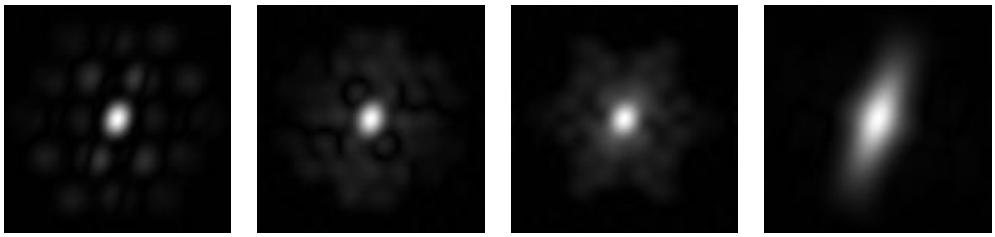

(a) Annulus (b) Golay-6 (c) Tri-Arm (d) Equivalent Filled

Fig.7 MTF plots of three kinds of the typical array configurations of the sparse aperture systems with F=30% and their equivalent filled system, produced from the experimental PSFs, respectively

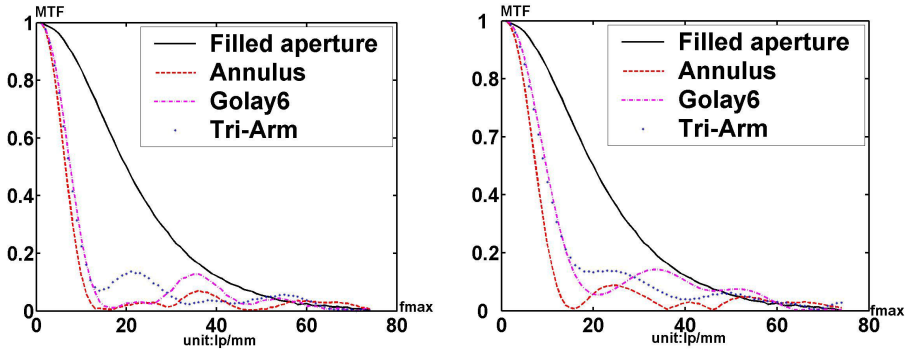

(a) F=20% (b) F=30%

Fig.8 Experimental MTF curves of three kinds of the typical array configurations of the sparse aperture systems and their equivalent filled system at the direction of the maximal cutoff frequency (Frequency unit: *lp/mm*)

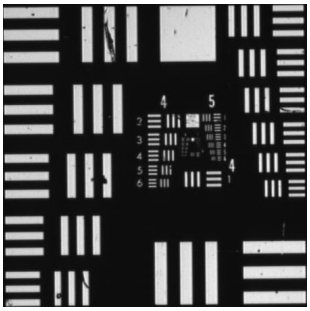

Fig.9 Imaging result from the equivalent filled system

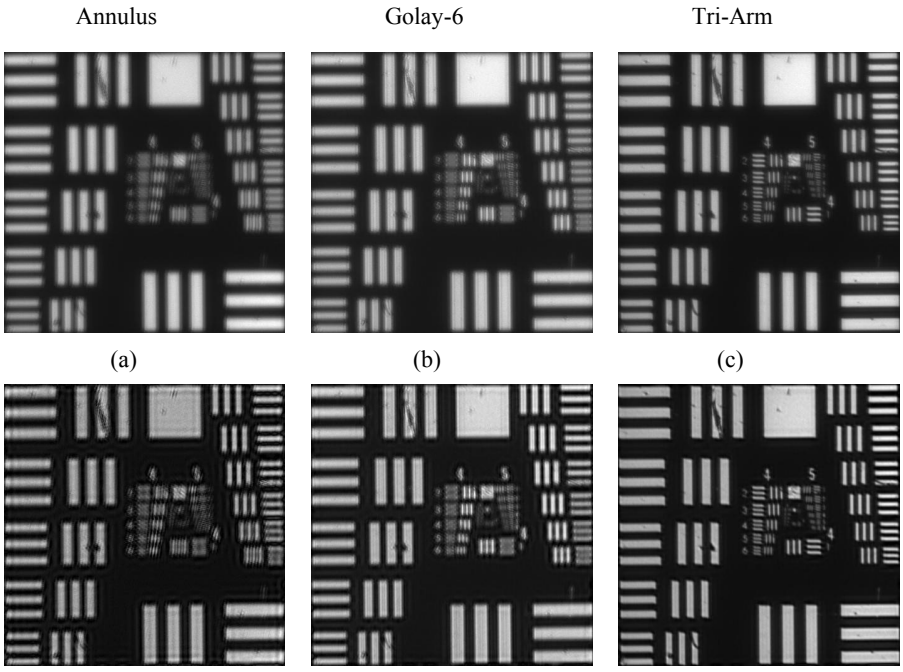

Fig10 Imaging results of three kinds of the typical array configurations of the sparse aperture systems (a) (b) (c) and the corresponding restored outputs with the Wiener filter (d) (e) (f)

Table.1 Correlation coefficients between the images of the sparse aperture systems and the images of the equivalent filled system at the different fill factor

Array Configuration	Image	F=20%	F=30%
Annulus	Direct Image	0.9032	0.9295
	Restored Image	0.9408	0.9574
Golay-6	Direct Image	0.8958	0.9233
	Restored Image	0.9325	0.9461
Tri-Arm	Direct Image	0.9217	0.9600
	Restored Image	0.9670	0.9770

4. CONCLUSIONS

According to the theoretical analysis, a principle experiment is set up for the optical sparse aperture imaging system. The imaging of the extended complex object is achieved. The image restoration of the direct outputs by the sparse aperture systems is performed by measuring the PSFs and by using the Weiner filter. The correlation coefficient is proposed as the criterion to determine the optimal parameter, and to evaluate the performance of the algorithms. The results show that the Tri-Arm array configuration among the three kinds of the typical configuration models can produce higher resolution and larger correlation coefficient value. Accordingly, based on the experimental data, the possibility is demonstrated that the optical sparse aperture imaging systems can achieve almost the same resolution and the image quality as an equivalent filled imaging system, which matches the results of the numerical simulations. In the experiments, we use the aperture masks to make the sub-apertures in the same plane, and the co-phasing condition of independent small aperture systems is satisfied inherently. In the near future, we will try to include the effects of the phasing errors for the image quality by establishing the sparse aperture imaging system with the independently adjustable sub-apertures.

ACKLNOWLEDEMENTS

Financial support by the National Natural Science Foundation of China (NSFC) (Contract No.60577029) is gratefully acknowledged. The authors also thank the financial support by the Funding Project for Academic Human Resources Development in Institutions of Higher Learning Under the Jurisdiction of Beijing Municipality (PHRIHLB). When this work was performed, Dayong Wang was with the Institut für Technische Optik, Universität Stuttgart, Pfaffenwaldring 9, D-70569 Stuttgart, Germany.

REFERENCES

1. Soon-Jo Chung, David W. Miller, Olivier L. de Weck. “ARGOS testbed: study of multidisciplinary challenges of future spaceborne interferometric arrays”, *Opt. Eng.* 43(9), 2156-2167 (2004).

2. R. L. Kendrick, Jean-Noel Aubrun, Ray Bell, et al., “Wide-field Fizeau imaging telescope: experimental results”, *Appl. Opt.* 45(18), 4235-4240 (2006).

3. Erin E. Sabatke, James H. Burge, and Philip Hinz ,“Optical design of interferometric telescopes with wide fields of view”, *Appl. Opt.* 45(31), 8026-8035 (2006).

4. Rick Kendrick, Eric H. Smith et al., “Multiple-aperture imaging spectrometer: computer simulation and experimental validation”, *IEEE Proceedings of the 33rd Applied Imagery Pattern Recognition Workshop* (AIPR’04), 3-9 (2004).

5. Joe Pitman, Alan Duncan and David Stubbs et al., “Remote sensing space science enabled by the multiple instrument distributed aperture sensor (MIDAS) concept”, *Proc. SPIE*. 5555, 301-310 (2004).

6. Robert D. Fiete, Theodore A. Tantalo et al., “Image quality of sparse-aperture designs for remote sensing”, *Opt. Eng*. 41(8), 1957-1969 (2002).

7. Hedser van Brug, Bastiaan Oostdijck, “Homothetic mapping as means to obtain a wide field of view: the Delft testbed interferometer”, *Proc. SPIE*. 5491, 1598-1606 (2004).

8. Peter Giesen, Bas Ouwerkerk, “Mechanical setup for optical aperture synthesis for wide field imaging”, *Proc. SPIE*. 5528, 361-371 (2004).

9. Iouri Tcherniavski，Mojtaba Kahrizi, “Optimization of the optical sparse array configuration”, *Opt. Eng.* 44 (10), 103201-1~10 (2005).

10. H.F.A.Tschunko, P.J.Sheehan, “Aperture configuration and imaging performance”, *Appl. Opt.* 10(6), 1432-1438 (1971).

11. Quanying Wu, Lin Qian, “Imaging recovering for sparse-aperture system”, *Proc. SPIE*. 5624, 478-486 (2005).

12. Dayong Wang, Xiyang Fu et al., “Analysis of field-of-view of optical aperture synthesis imaging interferometry”, *Proc. SPIE*. 5636, 40-47 (2005).

13. Dayong Wang, Jun Chang and Hancheng Liu et al., “Wide-field imaging design and image restoration with optical sparse-aperture system”, *Proc. SPIE*. 6149, 61493B-1~61493B-7 (2006).

14. Joseph W. Goodman, *Introduction to Fourier Optics*, McGraw-Hill Companies, Inc., New York , Second Edition, 1996.

15. Rafael C. Gonzalez, Richard E. Woods. *Digital Image Processing*. Prentice Hall, Second Edition, 2003.